Available online at www.sciencedirect.com

ScienceDirect

Procedia Engineering 126 (2015) 431 – 435

Procedia Engineering

www.elsevier.com/locate/procedia

7th International Conference on Fluid Mechanics, ICFM7

Self-propulsion of a flexible plunging foil near a solid wall

Longzhen Dai*, Guowei He, Xing Zhang

LNM, Institute of Mechanics, Chinese Academy of Science, Beijing 100190, China

Abstract

This paper is a numerical investigation of wall effect on the self-propulsion of a flexible plunging foil. Simulations are performed by a Fluid-Structure Interaction (FSI) solver which couples immersed boundary method for the fluid and finite difference method for the structure. A systematic study is conducted by varying the distance between the foil and the wall. It is found that the time-averaged lift force first pulls the foil towards the wall and then pushes foil away from the wall as the distance decreases. The cruising speed increases when the foil approaches the wall, while the propulsive efficiency decreases a little and then increases rapidly as the distance becomes less than one chord length of the foil. It is observed that wake structure deflects obviously in the near-foil regions, but becomes parallel to the horizontal direction again in the far field downstream.

Peer-review under responsibility of The Chinese Society of Theoretical and Applied Mechanics (CSTAM)

Keywords: self-propulsion; flexible foil; plunging; wall effect; enhancement

1. Introduction

Wall effect, which is also referred as ground effect, is ubiquitous in bio-locomotion in nature. Representative examples are birds flying over water surfaces [1, 2], and fish swimming near the bottom [3]. Wall effect inevitably changes the propulsive performance of those propulsors. In recent years, several model problems have been studied, however, results were not quite in agreement with each other. In [4], it was found that swimming near the ground increased the propulsive efficiency of a flexible panel in some cases, and very often this panel swam faster near the ground. And in [5], it was observed that the wall could enhance the cruising velocity of a flexible foil up to 25%, and the optimal position from the wall was about 0.4 times the foil's chord length. In contrast, the study [6] found that the propulsive efficiency of a rigid aerofoil kept the same at different distances from the wall. Furthermore, another study [7] on a stingray-inspired flexible fin indicated that ground effect did not necessarily enhance the propulsive

* Corresponding author. Tel.: +86 10 82543927; fax: +86 10 82543977.
E-mail address: dailongzhen@imech.ac.cn

Peer-review under responsibility of The Chinese Society of Theoretical and Applied Mechanics (CSTAM)
doi:10.1016/j.proeng.2015.11.262

performance. Usually, the flexible fins did not swim faster in ground effect, the power requirements increased, and the cost of transport could increase by up to 10%. To summarize, substantial divergence of the wall effect on flapping swimmers appeared among previous studies. Meanwhile, to our knowledge, those studies were carried out using the experiments, and most of them imposed a free stream on the fixed propulsor.

In this paper, we use the self-propulsion of a flexible foil in still fluid near a solid wall to model the swimming of a fish under side-wall effect. Systematic numerical simulations are carried out by varying the distance between the foil and the wall. Our work is primarily designed to answer two questions: (1) does the wall effect really enhance the performance of flapping swimmers; (2) what are the effects of wall on the wake structure behind the swimmers?

2. Model problem and numerical set-up

For the model problem, the fluid flow is two-dimensional, incompressible and initially still; the flexible foil is treated as an inextensible filament, and is actuated by the plunging motion of its leading edge. It implies that the leading edge undergoes a periodical oscillation in the vertical direction, but free to move horizontally with its angle of orientation parallel to the *x*-axis. In this paper, the plunging motion is prescribed as $Y(t) = A\cos\omega t$, where A and ω are the plunging amplitude and circular frequency respectively. Fig. 1 is a schematic diagram of the flexible foil near a solid wall. Here, c is the chord length of the foil; d is the vertical distance between the leading edge and the wall. The dimensionless plunging amplitude and wall distance are defined as $\overline{A} = A/c$ and $D = d/c$, respectively.

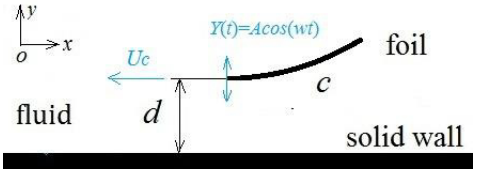

Fig. 1. Schematic diagram of the flexible foil near a solid wall.

Motions of the fluid and the foil are governed by the Navier-Stokes equations and the non-linear structural equations which are written in the dimensionless form as (1) and (2), respectively. The two equations are obtained by scaling space with c and time with c/U_{ref}, where $U_{ref} = A\omega$ is the reference velocity. In Eq. (1), $\vec{u}$ is the fluid velocity; p is the fluid pressure; Re_p is the plunging Reynolds number; $\vec{f}$ is the Eulerian forcing term used to mimic the effect of immersed foil on the fluid flow. In Eq. (2), $\vec{X}$ is the position vector; s is the Lagrangian coordinate along the arc length; $\vec{F}$ is the Lagrangian forcing term due to the interaction between foil and fluid; β, ζ, γ are the mass ratio of the foil to the fluid, dimensionless tension coefficient and bending rigidity respectively.

$$\begin{cases} \dfrac{\partial \vec{u}}{\partial t} + \nabla\cdot\left(\vec{u}\vec{u}\right) = -\nabla p + \dfrac{1}{\mathrm{Re}_p}\nabla^2\vec{u} + \vec{f} \\ \nabla\cdot\vec{u} = 0 \end{cases} \tag{1}$$

$$\begin{cases} \beta\dfrac{\partial^2\vec{X}}{\partial t^2} = \dfrac{\partial}{\partial s}\left(\zeta\dfrac{\partial\vec{X}}{\partial s}\right) - \dfrac{\partial^2}{\partial s^2}\left(\gamma\dfrac{\partial^2\vec{X}}{\partial s^2}\right) - \vec{F} \\ \dfrac{\partial\vec{X}}{\partial s}\cdot\dfrac{\partial\vec{X}}{\partial s} = 1 \end{cases} \tag{2}$$

A loosely-coupled fluid-structure interaction (FSI) solver is used to simulate the model problem. In the FSI solver, the flow solver and structure solver are alternatively advanced by one step in time. In the flow solver, the governing equations of fluid (Eq. (1)) are numerically solved by using the direct-forcing immersed boundary method based on the discrete stream function formulation for incompressible Navier-Stokes equations [8]. In the structure solver, the governing equations of flexible foil (Eq. (2)) are solved by a finite difference method based on a staggered grid. Details and validations of the structure solver and the FSI solver were provided in [9].

Numerical simulations are performed in a rectangular domain of size [-20c, 20c]×[-6c, 6c], with the minimum mesh size 0.02c. The solid wall is located at the bottom line y =-6c, x= [-20c, 20c]. The foil is uniformly meshed with size 0.02c, and is represented by 51 Lagrangian points. Non-slip boundary conditions are imposed on the solid wall and the immersed foil, while free-slip boundary conditions are imposed on other three boundaries of the computational domain. Input parameters are chosen as: $\mathrm{Re}_f = 100$, $\beta = 2.0$, $\bar{A} = 0.1$, $\gamma = 6.0$. A series of distances D are investigated as shown in Table 1. The smaller the value D, the stronger the wall effect. However, values smaller than 0.4 are not included in our simulations, because the foil starts to touch the wall and numerical calculations cannot continue any more when D becomes less than 0.4.

Table 1. Series of value D used in the simulations.

Case	1	2	3	4	5	6	7	8	9	10	11	12	13	14
D	0.4	0.45	0.5	0.6	0.7	0.8	0.9	1.0	1.2	1.5	2.0	3.0	4.0	6.0

3. Results and discussions

In order to study wall effect, four important parameters related to the propulsive performance need to be defined. They are: the time-averaged force $\vec{F}_{total}$, the cruising speed U_c, the swimming power P_s and the propulsive efficiency η. Parameters U_c, P_s are defined as the average horizontal velocity reached by the leading edge of the foil and the average input power required to produce the oscillation of the foil in one plunging period, respectively. The mathematical formulas of the four parameters are written as

$$\begin{cases} \vec{F}_{total} = 2 \cdot \int_0^{T_p} \left(\int_0^1 \vec{F} ds \right) dt, \quad U_c = -\frac{1}{T_p} \int_0^{T_p} \left(\frac{\partial X_{s=0}}{\partial t} \right) dt \\ P_s = \frac{1}{T_p} \int_0^{T_p} \left(\int_0^1 \left(\vec{F} \cdot \frac{\partial \vec{X}}{\partial t} \right) ds \right) dt, \quad \eta = \frac{\frac{1}{2} \beta U_c^2}{T_p P_s} \end{cases} \tag{3}$$

where T_p is the dimensionless plunging period, and $X_{s=0}$ is the horizontal position of leading edge.

3.1. Wall effect on forces and propulsive performance

Fig. 2 (a) shows the time-averaged forces $\vec{F}_{total} = \left(F_{x\_aver}, F_{y\_aver} \right)$ of the foil as a function of distance D at the periodically steady state. Due to the condition of "self-propulsion", F_{x_aver} is zero in all cases. In contrast, F_{y_aver}, i.e. the time-averaged lift force, changes greatly and is found to have two distinct regimes. For cases 0.6<D<6.0, the average lift force is negative and tends to pull the foil towards the wall; for cases 0.4≤ D≤0.6, the average lift force is positive and tends to push the foil away from the wall. There is an equilibrium point at D≈0.6 where the time-averaged lift is zero. This interesting phenomenon has also been reported in reference [1]. According to our data, instantaneous lift force is positive in the downstroke and negative in the upstroke during one plunging

period. Both of their magnitudes increase as the foil moves close to the wall. When D decreases to 0.6, the negative one increases more rapidly, thus average lift is negative. When D further decreases to 0.4, the positive one increases more rapidly, thus the average lift is positive. At the equilibrium point $D\approx0.6$, the negative one is equal to the positive one, so the average lift is zero.

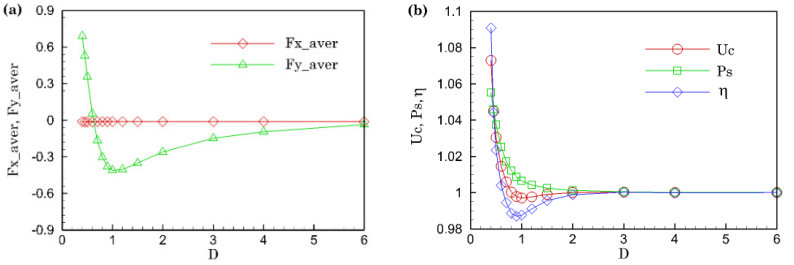

Fig. 2. (a) Time-averaged forces of the flexible foil in x- and y-directions as a function of distance D; (b) Cruising speed, swimming power and propulsive efficiency at different values of D.

Fig. 2 (b) shows the cruising speed, swimming power and propulsive efficiency as a function of distance D. All quantities in the vertical coordinate are normalized by the values obtained in case D=6.0. It is found that the three parameters exhibit no obvious variation from the values in D=6.0 if $D\geq3.0$. When D decreases from 3.0 to 0.4, cruising speed increases at the cost of the rising swimming power, while propulsive efficiency first declines a little and then increases rapidly when $D<1.0$. This behavior of propulsive efficiency is due to the different increasing rates of cruising speed and swimming power at different distances. When D changes from 3.0 to 1.0, the swimming power increases slightly while cruising speed almost keeps the same. Therefore, according to Eq. (3), the propulsive efficiency decreases in this range of D. When distance D decreases further from 1.0 to 0.4, cruising speed increases faster than swimming power, which leads to the substantial enhancement of propulsive efficiency in these regions. At the distance of D=0.4, the enhancement of cruising speed reaches 7.3%, at the cost of a 5.5% swimming power increase. Consequently, the propulsive efficiency receives an enhancement of 9.1%.

3.2. Wall effect on wake structures

To study the wall effect on wake structure, three representative plots of instantaneous vorticity contours are given in Fig. 3, where (a), (b) and (c) are corresponding to the cases D=6.0, 0.7 and 0.4, respectively. In plots (b) and (c), the solid wall is located at the bottom edge of the contour region, i.e. y= -6, while in plot (a) it is too far to be included. Enlarged plots of a vortex dipole in the rectangular box are provided at the right side for convenience.

For case D=6.0 (Fig. 3(a)), the vortices shed from trailing edge form a typical reverse von Karman vortex street. When the foil moves towards the wall to the position D=0.7 (Fig. 3(b)), vortices of considerable strength are produced and shed from the wall in near-foil regions. They are of the opposite sign to the vortices shed from the foil.

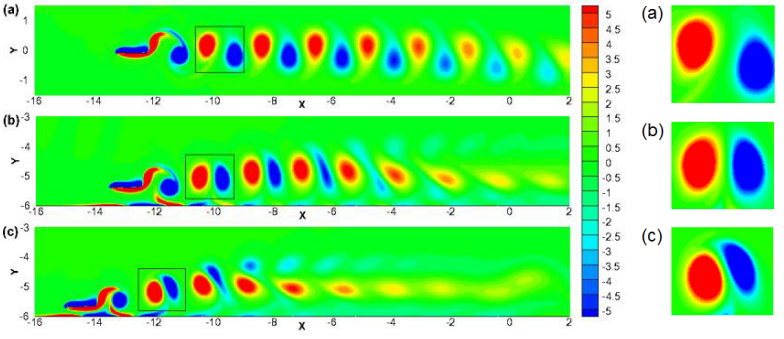

Fig. 3. Instantaneous vorticity contours at distance (a) D=6.0; (b) D=0.7; (c) D=0.4.

Specifically, clockwise vortex (with negative vorticity and blue color) leads to the production of anti-clockwise vortex (with positive vorticity and red color) after interacting with the wall, and vice versa. The smaller the distance between wake vortex and wall, the stronger the vortex produced on the wall. Meanwhile, the two counter-rotating vortices in a vortex dipole (the rectangular box in the plot) rotate as a whole in the anti-clockwise direction. Compared with (a), they stay closer to each other, and are stretched by the wall effect on their way downstream. The phenomena of stretching is more remarkable for the clockwise vortex, since it is shed at a position closer to the wall. When the foil moves to the position D=0.4, all the effects presented in (b) become much stronger. At this distance, the wake vortex develops into an asymmetric structure as shown in Fig. 3(c). Due to the strengthened anti-clockwise rotation of vortex pairs, the near wake becomes oblique with a small but noticeable deflection angle. However, the far wake turns back to be horizontal, after being heavily stretched and dissipated.

4. Conclusions

In order to study the wall effect on the propulsion of flexible flapping swimmers, we have conducted a series of numerical simulations by varying the distance between the flexible foil and the wall, while other input parameters are kept constant.

It is found that the wall effect could enhance the performance of plunging foil to some extent. According to our data, when foil moves close to the wall, cruising speed becomes larger at the cost of the increasing swimming power. However, cruising speed grows faster than swimming power when the distances are less than one chord length of the foil. Under such circumstances, propulsive efficiency also increases as distance becomes smaller, and its enhancement reaches 9.1% at the distance of 0.4 times the chord length of the foil. It is also interesting to find that the time-averaged lift first pulls the foil towards the wall and then pushes it away from the wall as the foil gradually approaches the wall.

It is observed that wake structure has changed greatly from the reverse Karman vortex street to an asymmetric pattern under the wall effect. When foil moves close to the wall, the vortex pair shed in one plunging period rotate as a whole in the clockwise direction, and meanwhile being stretched and dissipated rapidly on their way downstream. Therefore, wake structure deflects obviously in the near-foil regions, but turns back parallel to the propulsive direction in the far field.

Acknowledgements

This work is supported by Chinese Academy of Sciences under Project No. KJCX-SW-L08 and KJCX3-SYW-S01, National Natural Science Foundation of China under Project No. 11021262, No. 11023001, No. 11232011, No. 11372331. We would like to thank the National Supercomputing Center in Tianjin (NSCC-TJ) for the allocation of computing time.

References

[1] F. R. Hainsworth, Induced drag saving from ground effect and formation flight in brown pelicans, J. Exp. Bio. 135 (1988) 431-444.
[2] H. Weimerskirch, J. Martin, Y. Clerquin, P. Alexandre, S. Jiraskova, Energy saving in flight formation, Nature. 413 (2001) 697-698.
[3] P. W. Webb, Kinematics of plaice, *Pleuronectes platessa*, and cod, *Gadus morhua*, swimming near the bottom, J. Exp. Bio. 205 (2002) 2125-2134.
[4] D.B. Quinn, G.V. Lauder, A.J. Smits, Flexible propulsors in ground effect, Bioinspir. Biomim. 9 (2014) 1-8.
[5] R.F. Parts, V. Raspa, B. Thiria, F.H. Huarte, Large-amplitude undulatory swimming near a wall, Bioinspir. Biomim. 10(2015) 1-15.
[6] D.B. Quinn, K.W. Moored, P.A. Dewey, A.J. Smits, Unsteady propulsion near a solid boundary, J. Fluid Mech. 742 (2014) 152-170.
[7] E. Blevins, G.V. Lauder, Swimming near the substrate: a simple robotic model of stingray locomotion, Bioinspir. Biomim. 8 (2013) 1-12.
[8] S.Z. Wang, X. Zhang, An immersed boundary method based on discrete stream function formulation for two- and three-dimensinal incopressible flows, J. Comput Phys. 230 (2011) 3479-99.
[9] X. J. Zhu, G. W. He, X. Zhang, Numerical study on hydrodynamic effect of flexibility in a self-propelled plunging foil, Computers & Fluids. 97 (2014) 1-20.